

RESEARCH ARTICLE

View Article Online
View Journal | View IssueCite this: *Org. Chem. Front.*, 2026, **13**, 2024

Electrochemical deuteration of allylic esters with divergent site-selectivity

Xu Zhang,^{†a} Ke Liu,^{†a} Mohan Wang,^{†b} Chao Wu,^a Xiaoli Wang,^b Man-Bo Li ^a and Sheng Zhang ^{*a}

Deuterium-labelling technology has emerged as a promising new direction for drug discovery. Developing a divergent protocol to incorporate deuterium into different sites of bioactive molecules is highly desirable, as it opens up diverse access for leading compounds. Herein, we developed a site-selective divergent protocol for the deuteration of allylic esters *via* an electrochemical reduction approach. In the transformation, the reaction solvents and cathodes jointly dictated the reaction mechanism and active intermediates, and led to D₃-incorporation and mono-deuteration products. The synthetic utility of the electrochemical protocol is highlighted in the synthesis of D-labelled ACP synthase inhibitors. Further mechanistic studies involving linear sweep voltammetry (LSV) and gas chromatography (GC) confirmed that the observed selectivity originates from distinct reaction pathways.

Received 30th December 2025,
Accepted 4th February 2026

DOI: 10.1039/d5qo01759a

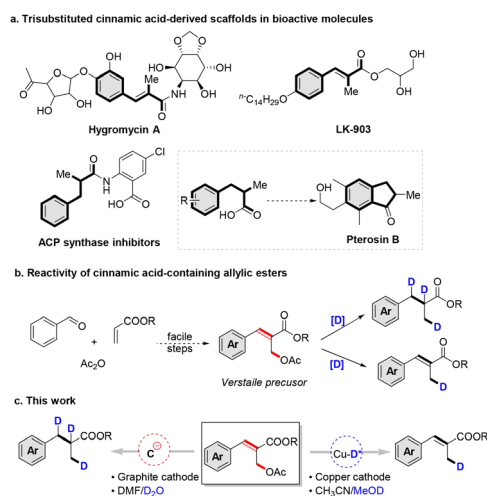
rsc.li/frontiers-organic

Introduction

Deuterium-containing compounds are of great significance in the fields of materials science, and physical and pharmaceutical chemistry.^{1–12} Consequently, considerable efforts have been devoted to discovering synthetic approaches. The explosive development of synthetic electrochemistry^{13–23} provides appealing opportunities for these transformations from commercially available deuterium sources, such as D₂O and CD₃CN. Amongst them, electroreductive deuteration of C=C bonds and C-heteroatom bonds are the major routes to D-labelled products. For instance, Zhang^{24,25} elegantly devised copper nanowire arrays for halide deuteration *via* the *in situ* formation of adsorbed metal-D species in the hydrogen evolution reaction (HER). Very recently, a novel rhodium nanocatalyst was disclosed by Lei and Li^{26,27} for highly selective alkene deuteration. Alternatively, carbanion-mediated deuteration for alkenes was developed independently by Cheng,⁵ Huang,²⁸ Qiu²⁹ and Werz³⁰ in the absence of catalysts. Moreover, the carbanion-mediated strategy was also applicable to halide/D exchange reactions, as demonstrated in the work of Qiu,³¹ Lin,³² Cheng³³ and Lennox.³⁴ Despite this impressive work, modulating site-selectivity in the deuteration of complex

substrates bearing both C=C and C-heteroatom bonds still faces great challenges but is highly desirable.

Trisubstituted cinnamic acid and its hydrogenated derivatives are prevalent scaffolds in bioactive molecules and facile building blocks for bioactive 1-indanones (Scheme 1a).^{35–39} Consequently, incorporating deuterium into these moieties might provide a diverse platform for deuterated leading compounds. Cinnamic-acid-containing allylic esters⁴⁰ can readily serve as versatile precursors for the corresponding D-labelled cinnamic acid and D₃-labelled products (Scheme 1b), owing to their multiple reaction sites (C=C, C–OAc). Nevertheless, the



Scheme 1 The utility and synthesis of trisubstituted cinnamic acid derivatives.

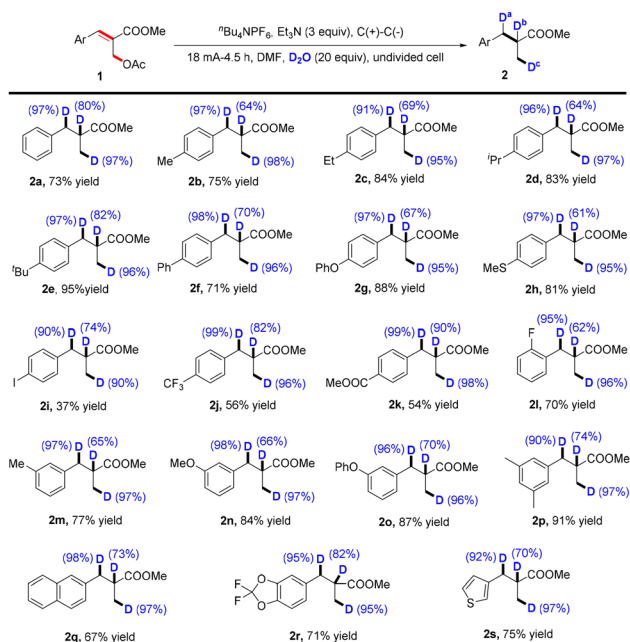
^aInstitutes of Physical Science and Information Technology, Key Laboratory of Structure and Functional Regulation of Hybrid Materials of Ministry of Education, Anhui University, Hefei, Anhui 230601, China. E-mail: shengzhang@ahu.edu.cn

^bSchool of Materials Science and Engineering, Anhui University, Hefei, Anhui 230601, China

[†]These authors contribute equally to this work.

inherent competing reaction is a major issue in the reaction. In particular, mono-selective deuteration *via* OAc/D exchange is elusive and uncultivated. With our long-term interest in carbanion chemistry and HER catalysis,^{41–49} we envisaged that electrochemical approaches might enable tunable access to these D-labelled products *via* the formation of carbanion or metal-D intermediates.

Precise control over the competing generation of carbanion and metal-D species in the reaction of allylic esters is key to accessing divergent D-labelled products. It is well known in energy chemistry that electrode materials dictate the overpotential for HER; metal cathodes (*e.g.* Pt, Cu) with lower overpotential would benefit HER compared to carbon materials.⁵⁰ Moreover, recent work by Lei and Li⁵¹ unveiled that the reaction solvent significantly affected the hydrogenation of polycyclic arenes by varying the proton migration rate. Inspired by this report, we have herein modulated the deuteration reaction pathway using different combinations of cathode and reaction solvents (Scheme 1c). With the evaluated reaction conditions, D₃-labelled and mono-deuterated products were selectively delivered. This protocol features good deuterium incorporation, divergent site-selectivity, broad substrate tolerance and reductant-free conditions. Several experiments, including linear sweep voltammetry (LSV) and gas chromatography (GC), were conducted to rationalize the divergent reaction pathway.

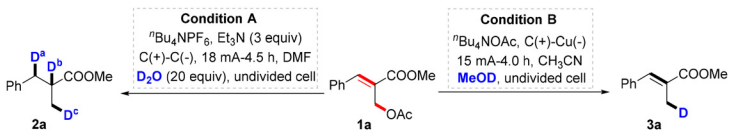


Scheme 2 Substrate generality of the electrochemical D₃-labelling reaction. Reaction conditions: **1** (0.5 mmol), ^tBu₄NPF₆ (1 mmol), Et₃N (1.5 mmol), graphite rod electrodes, DMF/D₂O (9.8/0.2 mL), undivided cell, constant current electrolysis (18 mA–4.5 h, 6.0 F mol⁻¹). D-incorporation of the product is determined by ¹H NMR. The yield listed is the isolated yield.

Results and discussion

We commenced our study by using allylic ester **1a** as the model substrate. D₃-labelled product **2a** was detected as the dominant product (entry 1, Table 1) with DMF as solvent, D₂O as D source, a graphite rod as the cathode, and Et₃N as an anodic sacrificial agent. Replacing DMF with THF led to lower yield and reduced D-incorporation in **2a**, while maintaining D₃-labelling selectivity (entry 2). Changing the cathode metal to Cu, Pb, or Zn under Condition A did not improve either the yield or the degree of D-incorporation compared with the standard conditions (entries 3–5). Using less acidic MeOD as the D source dramatically reduced the deuterium content (entry 6). It is noteworthy that D^a and D^c shared the same D-incorporation level, implying an allylic carbanion species in the reaction, as electron delocalization would give analogous D-incorporation at D^a and D^c sites. In contrast, the α-C–H bond of the ester (D^b) was less deuterated. This can be attributed to the reversibility of its deprotonation; despite its higher acidity, the resulting carbanion may be stabilized, leading to a slower or reversible deuterium incorporation step with D₂O. Removal of Et₃N led to a lower yield and showed a decline in D-incorporation (entry 7). The uniform preference for product **2a** showed that the multiple reaction sites of **1a** enable facile access to D₃-labelled products. To reverse this inherent reaction selectivity, we next screened various reaction conditions by varying the reaction solvent and cathode to CH₃CN and a copper plate, respectively. With a cheaper D source, MeOD, an allylic D-labelled product **3a** was exclusively afforded in 95% yield and 96% D-incorporation (entry 8). THF significantly affects the product distribution, giving a mixture of **2a** and **3a** (entry 9), which cannot be isolated by column chromatography. Further investigation on the cathode showed that cathode materials significantly affected the reaction site-selectivity. Graphite, lead and zinc cathodes resulted in substantial erosion in reaction selectivity (entries 10–12), while the HER-active cathode platinum retained selectivity for product **3a** (entry 13), although with lower yield (70%). When using D₂O as the D source, a slightly lower yield (84%) was observed (entry 14). Prolonging the reaction time to 6 hours afforded a major D₃-labelled product (entry 15), but it suffered from poor D-incorporation and low yield. Interestingly, the D distribution in the resulting product **2a** differed from that observed under **Condition B**, suggesting a different reaction mechanism.

With the optimal reaction conditions in hand, we examined the generality of the reaction. Initially, a collection of allylic esters was subjected to the D₃-labelling conditions (Scheme 2). This revealed that electron-rich substrates (**2a–2g**) slightly benefited the reaction efficiency compared to electron-deficient ones (**2h–2k**). Notably, conventionally sensitive functional groups, such as thioether, iodine, trifluoromethyl, and ester, were amenable to delivering the corresponding products (**2h–2k**). Specifically, the fact that the iodine atom is intact during the reaction excludes active hydride species in the reaction. Varying the substitution patterns was compatible in the electrochemical protocol, and the desired D₃-labelled products (**2l–2p**) were delivered in good yield (70–97%). Additionally, replacing the phenyl

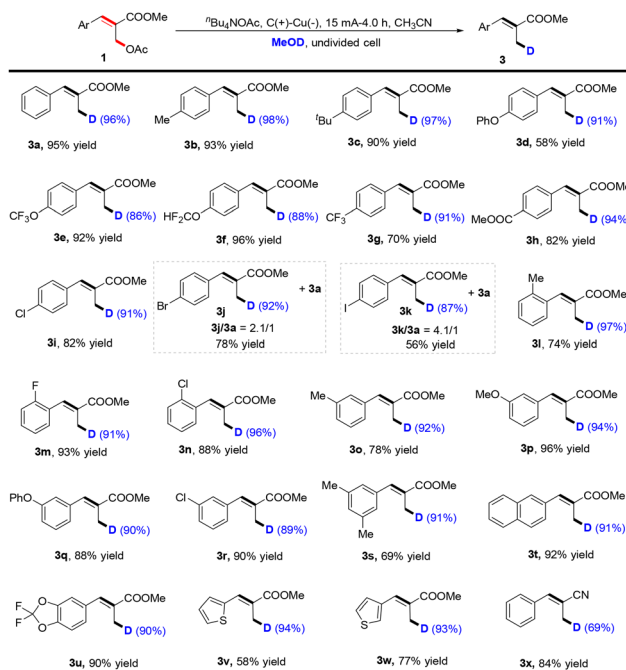
Table 1 Optimization of reaction conditions^a


Entry	Reaction conditions	Yield of 2a/3a ^b (%)	D-incorporation (2a) ^b	D-incorporation (3a) ^b
1	Condition A	73/trace	97%/80%/97%	n.d.
2	THF as solvent in Condition A	60/trace	94%/70%/94%	n.d.
3	Cu as cathode in Condition A	54/trace	90%/58%/93%	n.d.
4	Pb as cathode in Condition A	40/trace	93%/68%/78%	n.d.
5	Zn as cathode in Condition A	59/trace	95%/71%/97%	n.d.
6	MeOD as D source in Condition A	81/trace	70%/45%/72%	n.d.
7	Remove Et ₃ N from Condition A	52/trace	94%/80%/90%	n.d.
8	Condition B	Trace/95	n.d.	96%
9	THF as solvent in Condition B	23/63	n.d.	88%
10	C as cathode in Condition B	68/14	93%/68%/85%	n.d.
11	Pb as cathode in Condition B	30/57	n.d.	89%
12	Zn as cathode in Condition B	49/29	99%/73%/86%	93%
13	Pt as cathode in Condition B	Trace/70	n.d.	91%
14	D ₂ O as D source in Condition B	Trace/84	n.d.	95%
15	6 h in Condition B	56/3	92%/68%/81%	n.d.

^a **Condition A:** **1a** (0.5 mmol), ^tBu₄NPF₆ (1 mmol), Et₃N (1.5 mmol), graphite rod electrodes, DMF/D₂O (9.8/0.2 mL), undivided cell, constant current electrolysis (18 mA–4.5 h, 6 F mol⁻¹). **Condition B:** **1a** (0.5 mmol), ^tBu₄NOAc (1 mmol), graphite rod anode, copper plate cathode (1.8 × 2.0 cm²), CH₃CN/MeOD (9.0/1.0 mL), undivided cell, constant current electrolysis (15 mA–4.0 h, 4.5 F mol⁻¹). ^b The ratio of **2a/3a** and D-incorporation were determined by ¹H NMR.

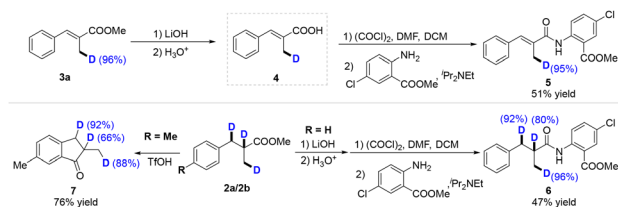
ring with fused rings (**2q–2r**) and thiophene largely maintained the reaction yield and D-incorporation. Nevertheless, the deuterium content of the α-C-site of the ester is uniformly lower than that at the other two sites, partly due to the lower reactivity of the carbanion species.

We next turned our attention to the mono-deuteration of allylic esters (Scheme 3). Generally, the protocol exhibits excellent tolerance for a broad range of functional groups, including phenoxy (**3d**), fluoroalkyl (**3e–3g**), ester (**3h**), and chlorine (**3i**) groups. Investigation of electronic properties reveals that an electron-rich phenoxy group (**3d**) led to lower efficiency compared to electron-deficient ones (**3e–3f**), but higher D-incorporation (91%). Nevertheless, strongly electron-deficient substrates **3g–3h** resulted in diminished yield. It is noteworthy that the deuteration of bromine- and iodine-substituted substrates at a copper cathode delivered the resulting C–O cleavage products (**3j–3k**) with a substantial amount of dehalogenation product. This observation evidenced Cu–D species in the reaction. The effect of substitution patterns was subsequently investigated. *ortho*-, *meta*- and multiple substitution patterns were well tolerated to give the corresponding products (**3l–3s**) in good yield and high deuterium content (89–97%). Fused rings and heterocycles were also subjected to the optimal reaction conditions, which were precisely deuterated to deliver D-labelled products **3t–3w** with excellent D-incorporation (90–94%). Nevertheless, an electron-rich thiophene ring (**3v–3w**) reduced the reaction yield, presumably due to the stronger C–OAc bond. Finally, an acrylonitrile-derived substrate proved to be amenable to give mono-deuterated product **3x**, albeit with lower D-incorporation.



Scheme 3 Substrate generality of electrochemical mono-deuteration. Reaction conditions: **1** (0.5 mmol), ^tBu₄NOAc (1 mmol), graphite rod anode, copper plate cathode (1.8 × 2.0 cm²), CH₃CN/MeOD (9.0/1.0 mL), undivided cell, constant current electrolysis (15 mA–4.0 h, 4.5 F mol⁻¹). D-incorporation of the product is determined by ¹H NMR. The yield listed is isolated yield.

After evaluating the reaction generality, the synthetic utility of the present protocol was investigated (Scheme 4). We employed the deuterated products in the precursor synthesis



Scheme 4 Investigation of synthetic utility.

of ACP synthase inhibitors. The D-labelled products **3a** and **2a** were subjected to sequential procedures involving facile ester hydrolysis and amidation. The desired products **5** and **6** were delivered in 51% and 47% yields, which can directly convert to ACP synthase inhibitors *via* a further ester hydrolysis. Additionally, the trifluoromethanesulfonic acid (TfOH)-mediated Friedel-Crafts acylation of D₃-labelled product **2b** enables direct access to bioactive 1-indanone **7**.

To gain insight into the reaction mechanism, a series of linear sweep voltammetry (LSV) and gas chromatography (GC) experiments were conducted (Fig. 1). Initially, LSV testing of both reaction systems revealed that the cathode materials and reaction solvents significantly affect the reduction behaviors of substrate **1a** and the deuterium source (Fig. 1a–b). At the graphite cathode, substrate **1a** is reduced more readily than D₂O (Fig. 1a), whereas at the copper cathode in acetonitrile,

MeOD reduction predominates over that of **1a**. These results collectively indicate the presence of two distinct reaction pathways (Fig. 1b). Direct reduction of **1a** initiates deuteration in the DMF solvent and graphite cathode *via* carbanion species. By contrast, the hydrogen evolution of MeOD starts the mono-deuteration of **1a** through an *in situ*-formed Cu–D intermediate. Subsequently, GC-monitoring experiments performed during the first hour of both reactions provided further evidence supporting the above conclusion (Fig. 1c–d). The results showed that only trace D₂ was detected in the D₃-labelling reaction (Fig. 1c), whereas a substantial amount of D₂ was observed in the mono-deuteration system (Fig. 1d). Finally, the oxidation behaviors of substrate **1a**, Et₃N, and ⁿBu₄NOAc were also investigated by cyclic voltammetry (CV), and the oxidations of Et₃N and ⁿBu₄NOAc were regarded as the major anodic reactions in D₃-incorporation and mono-deuteration (Fig. S25, p S17), respectively.

We further investigated the reaction mechanism by designing various control experiments (Fig. 2a–c). First, radical suppression experiments revealed that common radical scavengers, such as 1,1-diphenylethylene, 2,2,6,6-tetramethylpiperidinoxy (TEMPO) and *tert*-butanol, have a negligible effect on reaction efficiency, excluding the possibility of a radical-type mechanism (Fig. 2a). Second, using a combination of NaBH₄ and CuCl₂ to replace electrolysis led to a detectable product **3a-H**, supporting the Cu hydride species being

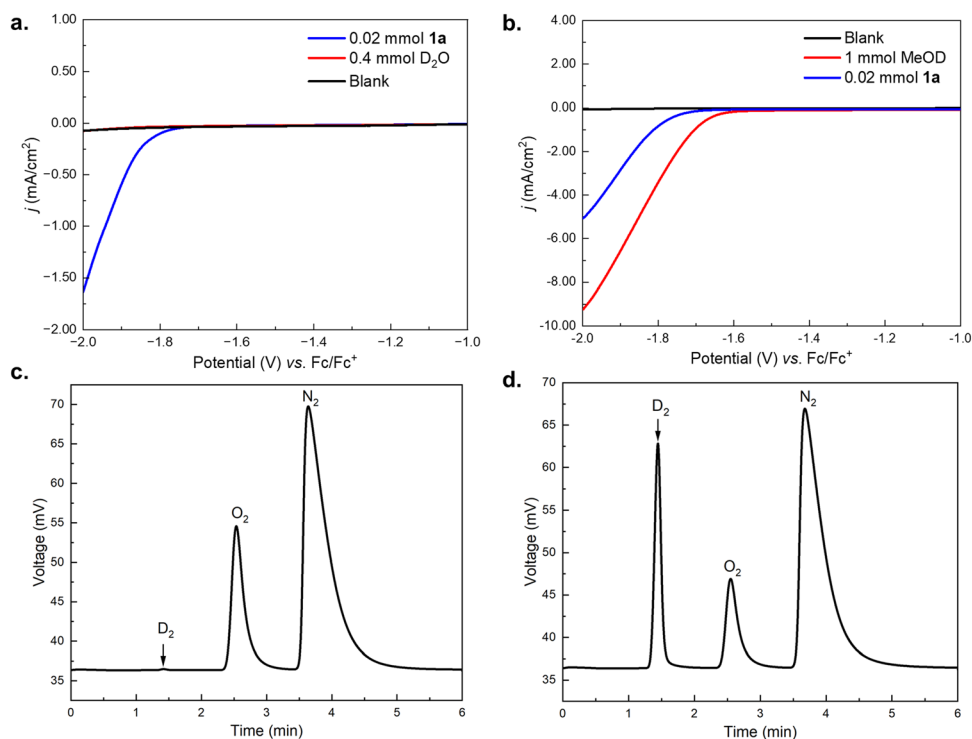


Fig. 1 (a) Linear sweep voltammograms of substrate **1a** and D₂O in DMF (0.1 M, ⁿBu₄NPF₆) using graphite, platinum wire and Ag/AgNO₃ as working, counter and referencing electrodes, respectively. (b) Linear sweep voltammograms of substrate **1a** and MeOD in CH₃CN (0.1 M, ⁿBu₄NOAc) using copper, platinum wire and Ag/AgNO₃ as working, counter and referencing electrodes, respectively. (c) GC spectra of the headspace atmosphere of the D₃-labelling reaction. (d) GC spectra of the headspace atmosphere of the mono-deuteration reaction.

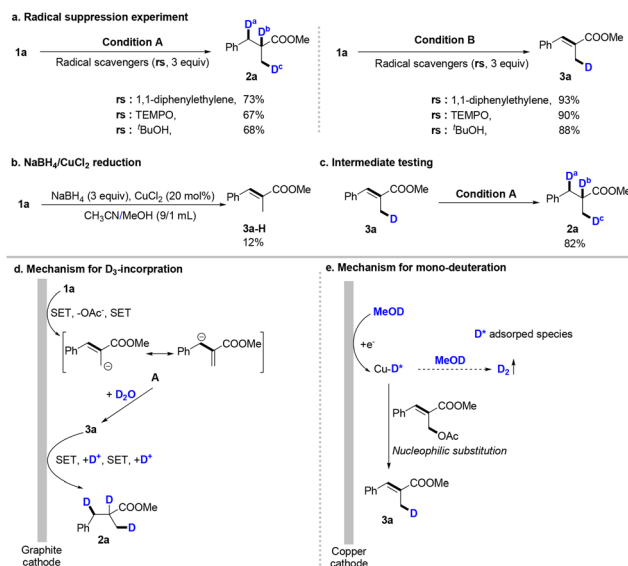


Fig. 2 Control experiments and proposed reaction mechanism.

involved in the mono-deuteration reaction (Fig. 2b). Third, the possible intermediate acrylates **3a** were subjected to the electrochemical D₃-labelling conditions (Fig. 2c). The high reaction yield and D-incorporation indicate that the D₃-labelling reaction should proceed *via* stepwise deuteration of intermediates **3a**.

On the basis of the experimental observations and related reports,^{5,29,31} two plausible pathways were proposed for electrochemical D₃-incorporation and mono-deuteration (Fig. 2d–e). In D₃-incorporation, substrate **1a** is initially reduced to carbanion species **A** *via* a sequential single electron transfer (SET), departure of OAc and SET. In the presence of excessive D₂O, rapid deuteration of carbanion **A** delivers intermediates **3a**, which undergo double sequences of SET and deuteration to give final D₃-labelled product **2a**. For the electrochemical mono-deuteration, the reduction of MeOD generates a reactive Cu–D species over the cathode. The Cu–D species serve as reactive nucleophiles to substitute an OAc group, giving mono-deuteration product **3a**. Alternatively, the neutralization of alkaline Cu–D with MeOD releases D₂ byproducts.

Conclusions

In conclusion, we developed an electrochemical protocol for the deuteration of allylic esters using commercially available deuterium source D₂O and MeOD. With variations in reaction solvents and cathodes, the reaction site-selectivity was readily tuned and divergent access to D₃-labelled and mono-deuterated products was enabled. Furthermore, we proposed two distinctive reaction pathways mediated by carbanion and Cu–D species to rationalize divergent selectivity. The further application of electrochemical deuteration approaches is being actively investigated in our lab.

Author contributions

S. Zhang and M.-B. Li conceived the project, designed the experiments, and wrote the manuscript. X. Zhang, K. Liu, M. Wang, C. Wu, X. Wang, and W. Fan performed the experimental work. All authors discussed the results and commented on the manuscript.

Conflicts of interest

There are no conflicts to declare.

Data availability

The data supporting this article have been included as part of the supplementary information (SI). Supplementary information: experimental details and characterization data for all new compounds. See DOI: <https://doi.org/10.1039/d5qo01759a>.

Acknowledgements

This work was supported by the National Natural Science Foundation of China (22571003, 22422101, 22371002) and the Anhui Provincial Natural Science Foundation (2308085Y14, 2508085ZD017).

References

- 1 K. B. Wiberga, The Deuterium Isotope Effect, *Chem. Rev.*, 1995, **55**, 713–743.
- 2 M. Gómez-Gallego and M. A. Sierra, Kinetic Isotope Effects in the Study of Organometallic Reaction Mechanisms, *Chem. Rev.*, 2011, **111**, 4857–4963.
- 3 D. J. Kushner, A. Baker and T. G. C. Dunstall, Pharmacological Uses and Perspectives of Heavy Water and Deuterated Compounds, *J. Physiol. Pharmacol.*, 1999, **77**, 79–88.
- 4 T. Pirali, M. Serafini, S. Cargnin and A. A. Genazzani, Applications of Deuterium in Medicinal Chemistry, *J. Med. Chem.*, 2019, **62**, 5276–5297.
- 5 X. Liu, R. Liu, J. Qiu, X. Cheng and G. Li, Chemical-Reductant-Free Electrochemical Deuteration Reaction using Deuterium Oxide, *Angew. Chem., Int. Ed.*, 2020, **59**, 13962–13967.
- 6 W. Li, J. Rabeah, F. Bourriquen, D. Yang, C. Kreyenschulte, N. Rockstroh, H. Lund, S. Bartling, A.-E. Surkus, K. Junge, A. Brückner, A. Lei and M. Beller, Scalable and Selective Deuteration of (Hetero)arenes, *Nat. Chem.*, 2022, **14**, 334–341.
- 7 P. L. Norcott, Current electrochemical approaches to selective deuteration, *Chem. Commun.*, 2022, **58**, 2944–2953.
- 8 L.-L. Liao, Z.-H. Wang, K.-G. Cao, G.-Q. Sun, W. Zhang, C.-K. Ran, Y. Li, L. Chen, G.-M. Cao and D.-G. Yu,

- Electrochemical Ring-Opening Dicarboxylation of Strained Carbon–Carbon Single Bonds with CO₂: Facile Synthesis of Diacids and Derivatization into Polyesters, *J. Am. Chem. Soc.*, 2022, **144**, 2062–2068.
- 9 S. Kopf, F. Bourriquen, W. Li, H. Neumann, K. Junge and M. Beller, Recent Developments for the Deuterium and Tritium Labeling of Organic Molecules, *Chem. Rev.*, 2022, **122**, 6634–6718.
 - 10 X.-T. Min, Y.-K. Mei, B.-Z. Chen, L.-B. He, T.-T. Song, D.-W. Ji, Y.-C. Hu, B. Wan and Q.-A. Chen, Rhodium-Catalyzed Deuterated Tsuji–Wilkinson Decarbonylation of Aldehydes with Deuterium Oxide, *J. Am. Chem. Soc.*, 2022, **144**, 11081–11087.
 - 11 H. Li, M. Shabbir, W. Li and A. Lei, Recent Advances in Deuteration Reactions, *Chin. J. Chem.*, 2024, **42**, 1145–1156.
 - 12 B.-Z. Chen, D.-W. Ji, B.-C. Zhou, X.-Y. Wang, H. Liu, B. Wan, X.-P. Hu and Q.-A. Chen, Cobalt-catalyzed dehalogenative deuteration with D₂O, *Chin. J. Catal.*, 2024, **59**, 250–259.
 - 13 M. Yan, Y. Kawamata and P. S. Baran, Synthetic organic electrochemical methods since 2000: on the verge of a renaissance, *Chem. Rev.*, 2017, **117**, 13230–13319.
 - 14 Y. Jiang, K. Xu and C.-C. Zeng, Use of electrochemistry in the synthesis of heterocyclic structures, *Chem. Rev.*, 2018, **118**, 4485–4540.
 - 15 J.-i Yoshida, A. Shimizu and R. Hayashi, Electrogenerated cationic reactive intermediates: the pool method and further advances, *Chem. Rev.*, 2018, **118**, 4702–4730.
 - 16 K. D. Moeller, Using physical organic chemistry to shape the course of electrochemical reactions, *Chem. Rev.*, 2018, **118**, 4817–4833.
 - 17 S. R. Waldvogel, S. Lips, M. Selt, B. Riehl and C. J. Kampf, Electrochemical arylation reaction, *Chem. Rev.*, 2018, **118**, 6706–6765.
 - 18 Y. Yuan and A. Lei, Electrochemical oxidative cross-coupling with hydrogen evolution reactions, *Acc. Chem. Res.*, 2019, **52**, 3309–3324.
 - 19 P. Xiong and H.-C. Xu, Molecular Photoelectrocatalysis for Radical Reactions, *Acc. Chem. Res.*, 2025, **58**, 299–311.
 - 20 C. Ma, J.-F. Guo, S.-S. Xu and T.-S. Mei, Recent Advances in Asymmetric Organometallic Electrochemical Synthesis (AOES), *Acc. Chem. Res.*, 2025, **58**, 399–414.
 - 21 P. Li, Y. Wang, H. Zhao and Y. Qiu, Electroreductive Cross-Coupling Reactions: Carboxylation, Deuteration, and Alkylation, *Acc. Chem. Res.*, 2025, **58**, 113–129.
 - 22 P. Gandeepan, L. H. Finger, T. H. Meyer and L. Ackermann, 3d metallaelectrocatalysis for resource economical syntheses, *Chem. Soc. Rev.*, 2020, **49**, 4254–4272.
 - 23 L. F. T. Novaes, J. Liu, Y. Shen, L. Lu, J. M. Meinhardt and S. Lin, Electrocatalysis as an enabling technology for organic synthesis, *Chem. Soc. Rev.*, 2021, **50**, 7941–8002.
 - 24 C. Liu, S. Han, M. Li, X. Chong and B. Zhang, Electrocatalytic Deuteration of Halides with D₂O as the Deuterium Source over a Copper Nanowire Arrays Cathode, *Angew. Chem., Int. Ed.*, 2020, **59**, 18527–18531.
 - 25 C. Liu, Y. Wu, B. Zhao and B. Zhang, Designed nanomaterials for electrocatalytic organic hydrogenation using water as the hydrogen source, *Acc. Chem. Res.*, 2023, **56**, 1872–1883.
 - 26 F. Bu, Y. Deng, L. Lu, Y. Li, W. Song, Z. Yang, X. Luo, X. Dong, R. Yi, D. Yang, S. Wang, A. Lei and W. Li, Electrocatalytic Alkene Hydrogenation/Deuteration, *J. Am. Chem. Soc.*, 2025, **147**, 5785–5795.
 - 27 F. Bu, Y. Deng, J. Xu, D. Yang, Y. Li, W. Li and A. Lei, Electrocatalytic reductive deuteration of arenes and heteroarenes, *Nature*, 2024, **634**, 592–599.
 - 28 Y. Qin, J. Lu, Z. Zou, H. Hong, Y. Li, Y. Li, L. Chen, J. Hu and Y. Huang, Metal-free chemoselective hydrogenation of unsaturated carbon–carbon bonds via cathodic reduction, *Org. Chem. Front.*, 2020, **7**, 1817–1822.
 - 29 K. Yang, T. Feng and Y. Qiu, Organo-Mediator Enabled Electrochemical Deuteration of Styrenes, *Angew. Chem., Int. Ed.*, 2023, **62**, e202312803.
 - 30 S. Kolb and D. B. Werz, Site-selective Hydrogenation/Deuteration of Benzylic Olefins Enabled by Electroreduction Using Water, *Chem. – Eur. J.*, 2023, **29**, e202300849.
 - 31 P. Li, C. Guo, S. Wang, D. Ma, T. Feng, Y. Wang and Y. Qiu, Facile and general electrochemical deuteration of unactivated alkyl halides, *Nat. Commun.*, 2022, **13**, 3774.
 - 32 D. Wood and S. Lin, Deuterodehalogenation Under Net Reductive or Redox-Neutral Conditions Enabled by Paired Electrolysis, *Angew. Chem., Int. Ed.*, 2023, **62**, e202218858.
 - 33 J. Sheng and X. Cheng, Electrochemical Mono-Deuterodefluorination of Trifluoromethyl Aromatic Compounds with Deuterium Oxide, *CCS Chem.*, 2024, **6**, 230–240.
 - 34 J. R. Box, M. E. Avanthay, D. L. Poole and A. J. J. Lennox, Electronically Ambivalent Hydrodefluorination of Aryl-CF₃ groups enabled by Electrochemical Deep-Reduction on a Ni Cathode, *Angew. Chem., Int. Ed.*, 2023, **62**, e202218195.
 - 35 K. Isono, Current progress on nucleoside antibiotics, *Pharmacol. Ther.*, 1991, **52**, 269–286.
 - 36 S. Knapp, Synthesis of Complex Nucleoside Antibiotics, *Chem. Rev.*, 1995, **95**, 1859–1876.
 - 37 B. Das, J. Banerjee, N. Chowdhury and A. Majhi, Synthetic Applications of Baylis–Hillman Chemistry: An Efficient and Solely Stereoselective Synthesis of (*E*)- α -Methylcinnamic Acids and Potent Hypolipidemic Agent LK-903 from Unmodified Baylis–Hillman Adducts, *Chem. Pharm. Bull.*, 2006, **54**, 1725–1727.
 - 38 D. Joseph-McCarthy, K. Parris, A. Huang, A. Failli, D. Quagliato, E. G. Dushin, E. Novikova, E. Severina, M. Tuckman, P. J. Petersen, C. Dean, C. C. Fritz, T. Meshulam, M. DeCenzo, L. Dick, I. J. McFadyen, W. S. Somers, F. Lovering and A. M. Gilbert, Use of Structure-Based Drug Design Approaches to Obtain Novel Anthranilic Acid Acyl Carrier Protein Synthase Inhibitors, *J. Med. Chem.*, 2005, **48**, 7960–7969.
 - 39 M. Fukuoka, M. Kuroyanagi, K. Yoshihira and S. Natori, Chemical and Toxicological Studies on Bracken Fern,

- Pteridium aquilinum var. latiusculum. II. Structures of Pterosins, Sesquiterpenes having 1-Indanone Skeleton, *Chem. Pharm. Bull.*, 1978, **26**, 2365–2385.
- 40 X. Wang, K. Liu, X. Jin, X. Li, M. Shen, S. Zhang and M.-B. Li, Oxygen Atom Migration of Allylic Esters via an Organocatalyzed Claisen-type Rearrangement, *Eur. J. Org. Chem.*, 2025, e202401401.
- 41 S. Zhang, L. Li, J. Li, J. Xue, K. Xu, W. Gao, L. Zong, G. Li and M. Findlater, Electrochemical Arylation of Aldehydes, Ketones and Alcohols: from Cathodic Reduction to Convergent Paired Electrolysis, *Angew. Chem., Int. Ed.*, 2021, **60**, 7275–7282.
- 42 S. Zhang, J. Shi, J. Li, M.-B. Li, G. Li and M. Findlater, Catalyst-Dependent Direct and Deoxygenative Coupling of Alcohols by Convergent Paired Electrolysis, *CCS Chem.*, 2022, **4**, 1938–1948.
- 43 S. Zhang, W. Gao, J. Shi, J. Li, F. Li, Y. Liang, X. Zhan and M.-B. Li, Regioselective umpolung addition of dicyanobenzene to α,β -unsaturated alkenes enabled by electrochemical reduction, *Org. Chem. Front.*, 2022, **9**, 1261–1266.
- 44 S. Zhang, Y. Liang, K. Liu, X. Zhan, W. Fan, M.-B. Li and M. Findlater, Electrochemically Generated Carbanions Enable Isomerizing Allylation and Allenylation of Aldehydes with Alkenes and Alkynes, *J. Am. Chem. Soc.*, 2023, **145**, 14143–14154.
- 45 Y. Liang, J. Feng, H. Li, X. Wang, Y. Zhang, W. Fan, S. Zhang and M.-B. Li, A Hydrogen Evolution Catalyst [Co₂O₂] Metallacycle Enables Regioselective Allene C(sp²)-H Functionalization, *Angew. Chem., Int. Ed.*, 2024, **63**, e202400938.
- 46 K. Liu, M. Lei, X. Li, X. Zhang, Y. Zhang, W. Fan, M.-B. Li and S. Zhang, Paired electrocatalysis unlocks cross-dehydrogenative coupling of C(sp³)-H bonds using a pentacoordinated cobalt-salen catalyst, *Nat. Commun.*, 2024, **15**, 2897.
- 47 S. Zhang and M.-B. Li, Repurposing HER catalysis toward metal hydride-mediated electro-reductive transformations, *Tetrahedron Chem*, 2024, **11**, 100080.
- 48 J. Feng, Y. Xia, M. Shen, J. Wang, W. Fan, S. Zhang and M.-B. Li, Electrochemical Allene C–H Functionalization via Carbanion Sampling, *Angew. Chem., Int. Ed.*, 2025, **64**, e202508369.
- 49 S. Zhang, L. Hong, J. Feng, M. Wang, J. Hu, Y. Zhang and M.-B. Li, Bimetallic [Co/K] hydrogen evolution catalyst for electrochemical terminal C–H functionalization, *Nat. Commun.*, 2025, **16**, 8435.
- 50 Z. W. Seh, J. Kibsgaard, C. F. Dickens, I. Chorkendorff, J. K. Nørskov and T. F. Jaramillo, Combining Theory and Experiment in Electrocatalysis: Insights into Materials Design, *Science*, 2017, **355**, eaad4998.
- 51 H. Li, Y. Li, J. Chen, L. Lu, P. Wang, J. Hu, R. Ma, Y. Gao, H. Yi, W. Li and A. Lei, Scalable and Selective Electrochemical Hydrogenation of Polycyclic Arenes, *Angew. Chem., Int. Ed.*, 2024, **63**, e202407392.